ELSEVIER

Journal of Hazardous Materials B123 (2005) 262–268

Journal of Hazardous Materials

www.elsevier.com/locate/jhazmat

Arsenic removal by adsorption on iron(III) phosphate

Véronique Lenoble, Christelle Laclautre, Véronique Deluchat, Bernard Serpaud, Jean-Claude Bollinger*

Laboratoire des Sciences de l'Eau et de l'Environnement, Faculté des Sciences, 123 avenue Albert Thomas, 87 060 Limoges, France

Received 3 December 2004; received in revised form 8 April 2005; accepted 18 April 2005
Available online 17 May 2005

Abstract

Under natural conditions, arsenic is often associated with iron oxides and iron(III) oxidative capacity towards As(III) is well known. In this study, As(III) and As(V) removal was performed using synthesised iron(III) phosphate, either amorphous or crystalline. This solid can combine (i) As(III) oxidation by iron(III) and (ii) phosphate substitution by As(V) due to their similar properties. Results showed that adsorption capacities were higher towards As(III), leading to Fe^{2+} and $HAsO_4^{2-}$ leaching. Solid dissolution and phosphate/arsenate exchange led to the presence of Fe^{3+} and PO_4^{3-} in solution, therefore various precipitates involving As(V) can be produced: with Fe^{2+} as $Fe_3(AsO_4)_2{\cdot}8H_2O_{(s)}$ and with Fe^{3+} as $FeAsO_4{\cdot}2H_2O_{(s)}$. Such formations have been assessed by thermodynamic calculations. This sorbent can be a potential candidate for industrial waste treatment, although the high release of phosphate and iron will exclude its application in drinking water plants.

Keywords: Arsenic; Adsorption; Iron(III) phosphate

1. Introduction

Arsenic is a ubiquitous element found in the atmosphere, soils and rocks, natural waters and organisms [1]. It is mobilised through a combination of natural processes such as weathering reactions, biological activity and volcanic emissions as well as through a range of anthropogenic activities [2]. Most environmental arsenic problems are the result of mobilisation under natural conditions. However, man has an additional impact through gold mining, combustion of fossil fuels and the use of arsenical pesticides and herbicides [2], or of additives to livestock feed [3]. Although the use of arsenic-containing products such as pesticides and herbicides has decreased significantly in the last few decades, their use for wood preservation is still common [4]. The impact on the environment of the use of arsenic compounds, at least locally, will remain for some years. Of the various sources of arsenic in the environment, drinking water probably poses the greatest threat to human health and high arsenic concentrations can be found in groundwaters.

Following the accumulation of evidence for the chronic toxicological effects of arsenic in drinking water [5,6], the W.H.O. recommended that many authorities reduce their regulatory limits. In Europe (Directive 98/83/CE), and in the USA (http://www.epa.gov/safewater/ars/implement.html) for example, they were lowered from 50 to 10 μg total As/L. Processes to selectively remove the excess arsenic from both drinking water and industrial waste waters or mining discharges are therefore urgently required.

Removal of dissolved arsenic from water is linked to the chemistry of the As(III) and As(V) species and thus to their relative distribution, simultaneously influenced by pH and redox conditions [7,8]. In oxygen-rich environments where aerobic conditions persist, and under natural pH conditions, As(V) (arsenate) is prevalent and exists as a monovalent ($H_2AsO_4^-$) or divalent ($HAsO_4^{2-}$) anion, whereas As(III) (arsenite), the more toxic form, exists as an uncharged ($H_3AsO_3^0$) or anionic species ($H_2AsO_3^-$) in a moderately

* Corresponding author. Tel.: +33 555 457 469; fax: +33 555 457 459.
E-mail address: jcbollinger@unilim.fr (J.-C. Bollinger).

0304-3894/$ – see front matter © 2005 Elsevier B.V. All rights reserved.
doi:10.1016/j.jhazmat.2005.04.005

reducing environment where anoxic conditions persist [1,2].

Under natural conditions, arsenic is associated with iron oxides [9] and the formation of $Fe_3(AsO_4)_2{\cdot}8H_2O_{(s)}$ or $FeAsO_4{\cdot}2H_2O_{(s)}$ can be observed. Arsenic adsorption in soils increases with iron oxide content [10]. Furthermore, Fe(III) oxidative capacity towards As(III) is well known, especially when As(III) is adsorbed on the surface of iron oxide [11].

It is already known that arsenate and phosphate have similar chemical and biological properties [12] and this paper presents an economical, non-conventional material which combines Fe(III) oxidative capacity and the similar chemical properties of phosphate and As(V). A retention mechanism based on the study of phosphate release, to underline a possible exchange between phosphate and arsenate, and the thermodynamic prediction of precipitate formation are discussed.

2. Experimental

All chemicals were of analytical grade and used without further purification. All solutions were prepared with high purity de-ionised water (resistivity 18.2 MΩ cm) obtained with a Milli-Q water purification system (Elgastat Prima 1-3). All glassware was cleaned by soaking in 10% HNO_3 and rinsed three times with de-ionised water. The arsenate stock solution was prepared from sodium heptahydrate salt $Na_2HAsO_4{\cdot}7H_2O$ (Fluka, purity >98.5%). The arsenite stock solution was prepared from sodium (meta)arsenite $NaAsO_2$ (Fluka, purity >99%).

2.1. Iron(III) phosphate

Iron(III) phosphate was prepared as amorphous or crystallised solids, respectively named thereafter $FePO_{4(am)}$ and $FePO_{4(cr)}$. The amorphous $FePO_{4(am)}$ was prepared by mixing 50 mL of 0.83 M $FeCl_3$ (Prolabo, 29%) and 50 mL of 0.83 M $Na_3PO_4{\cdot}12H_2O$ (Prolabo, 98%), previously acidified to pH 1.2 with concentrated HCl [13]. As pH strongly decreased after mixing, it was fixed again to 1.2 with concentrated NaOH solution. After a standing time of 30 min, the brown precipitate was recovered by centrifugation (Sigma 2.15, Bioblock, 3215 × *g* during 10 min), washed with de-ionised water, air-dried for 1 day and ground for homogenisation. The crystalline $FePO_{4(cr)}$ was prepared according to the same protocol but using $Na_2HPO_4{\cdot}12H_2O$ (Prolabo, 99%) instead of Na_3PO_4; no thermal treatment was needed. The solids were stored in dark flasks and sheltered from light.

2.2. Solids characterisation

The solids' structures were analysed using X-ray Diffraction (Siemens D5000, with EVA 8.0 application included in the package) and Scanning Electronic Microscopy (Philips XL 30 combined to EDS analyser) techniques. Both Differential Thermal Analysis and ThermoGravimetric Analysis measurements were performed on a Setaram Labsys apparatus.

Specific surface areas were measured with the BET protocol (Micromeritics ASAP 2000). Surface charge and pH_{zpt} (pH value at zero point of titration) were determined by potentiometric titrations (PHM 250 Meterlab pH meter) of 1 g/L $FePO_4$ in 0.01 M $NaNO_3$ with 0.01 M NaOH and 0.01 M HNO_3 solutions [14]. Cationic exchange capacity (CEC) was established according to the NF X 31-130 standard [15]: a 10 g/L solid suspension was put in contact with a 4 g/L cobaltihexammine trichloride solution for 3 h. The difference in absorbance at 470 nm (measured with an Agilent 8453 spectrophotometer) between cobaltihexammine solution with and without solid led to the CEC value and thereafter to the surface pK_a [14].

2.3. Arsenic analysis

Total arsenic analyses were carried out using a Varian SpectrAA 800 graphite furnace atomic absorption spectrometer (GFAAS), with Zeeman background correction. All measurements were based on integrated absorbance using a hollow cathode lamp (Varian) at 193.7 nm. A palladium–magnesium mixture modifier was used, pretreatment temperature was 1400 °C and atomisation temperature was 2500 °C. The calibration range was 20–100 μg As/L, the accuracy was 5%, R.S.D. was ±7% (repeatability tests, $n > 100$).

2.4. Phosphate and iron colorimetric determination

Phosphate determination is based on the formation of an antimonyl-phosphomolybdate complex (Afnor standard NFT 90-023 based on ISO 6878-1: [16]), reduced with ascorbic acid to give a blue complex whose absorbance is measured at 700 or 880 nm according to the desired sensitivity. The use of a reductive mixture (sulphuric acid, sodium metabisulfite and sodium thiosulfate) prior to the antimonyl-phosphomolybdate complex formation prevents arsenate interference.

Iron determination is based on the red Fe^{2+}-orthophenantroline complex formation. Total iron or Fe^{2+} determination can be carried out with or without an ascorbic acid–based reductive mixture, respectively. Standards from 0 to 2.5 mg/L Fe^{2+} were prepared from a 1 g Fe^{2+}/L iron(II)-sulphate stock solution (Merck, 99.5%). The concentration of Fe^{2+} was determined by mixing 2.6 mL of sample to 0.8 mL of 0.05 M orthophenantroline chlorhydrate (Prolabo, 99.5%) and 2.5 mL of 5 M acetic acid (Prolabo, 100%) in a 25 mL-flask, filled with de-ionised water. Total iron concentration was determined according to the same protocol, but 2.6 mL of 1 M ascorbic acid (Aldrich, 99%) was also added. After a standing time of 1 h, absorbance was measured with an Agilent

8453 spectrophotometer at a wavelength of 510 nm in a 10-cm cell.

2.5. Adsorption experiments

The adsorption studies were performed separately on arsenite or arsenate solutions in the concentration range 0.5–100 mg/L. Experiments were carried out with a sorbent concentration of 1 g solid/L. Each solid was mixed at room temperature ($20 \pm 1\,^{\circ}C$) with the arsenic solution in closed flasks on an orbital shaker (Ikalabortechnik KS 501) at 200 rpm. Experiments were conducted without adjusting the pH of the solutions, i.e. at each matrix auto-equilibrium pH (pH drift less than 0.1 unit). Adsorption curves were realised in order to work out arsenic adsorption onto each matrix as a function of matrix auto-equilibrium pH and surface charge, and according to arsenite/arsenate speciation [7].

Table 1
Physico-chemical characteristics of $FePO_4$

	Amorphous $FePO_4$	Crystalline $FePO_4$
pH_{zpt}	3.7 ± 0.1	3.1 ± 0.1
Specific surface area (m^2/g)	53.6 ± 0.8	35.9 ± 0.5
CEC (mequiv./100 g solid)	44 ± 3	42 ± 3
Surface pK_a	7.4 ± 0.1	8.2 ± 0.1

3. Results

3.1. Solids characterisation

XRD and SEM analysis proved the amorphous or crystallised state of the two solids (Plate 1a and b, and Fig. 1). Each solid was pure as proven by the EVA 8.0 application. Physico-chemical properties (Table 1) indicate that cationic exchange capacities were the same but specific surfaces were different for the two solids: amorphous $FePO_4$ presents the

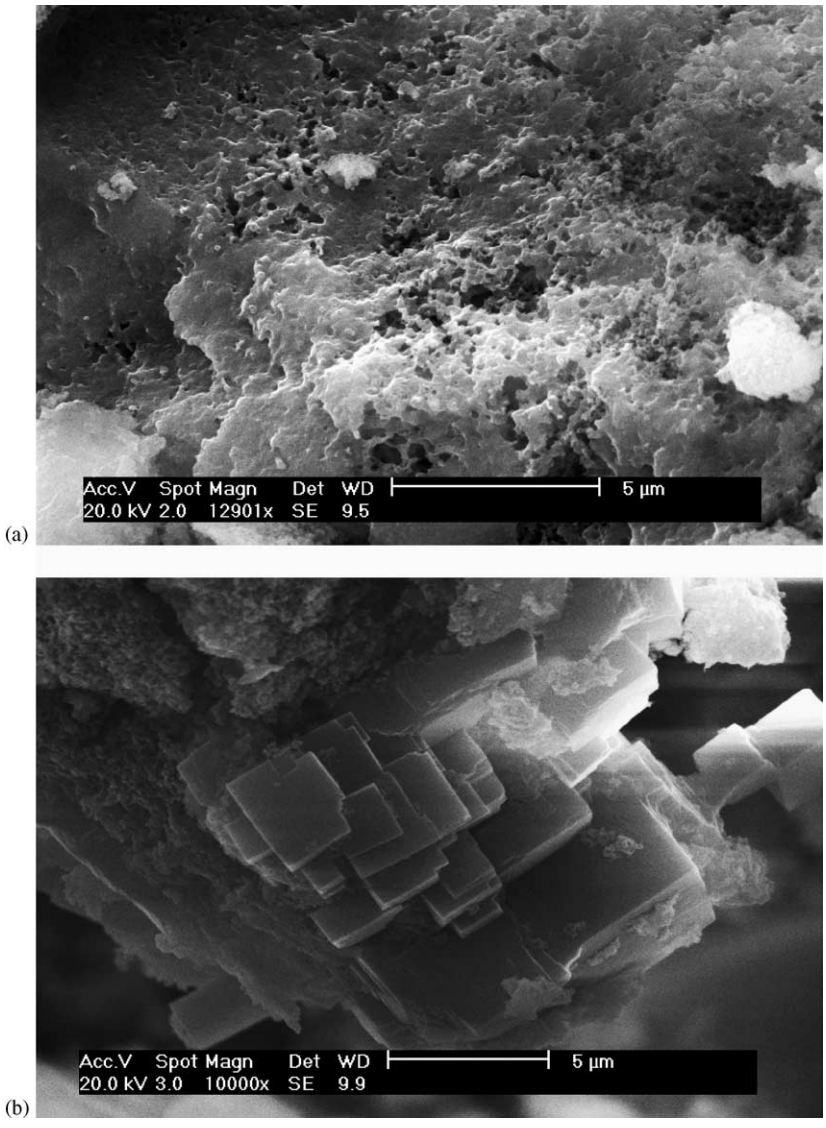

Plate 1. SEM analysis of $FePO_{4(am)}$ (a), and of $FePO_{4(cr)}$ (b).

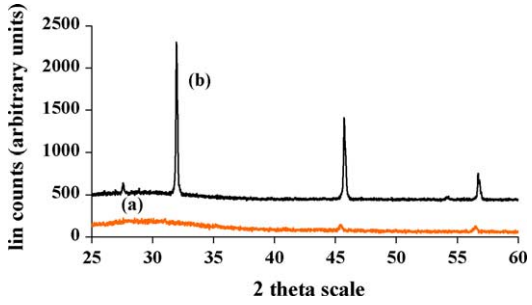

Fig. 1. XRD pattern for $FePO_{4(am)}$ (a) and $FePO_{4(cr)}$ (b), analysis between 28° and 58°, step size 0.040°, step time 6 s.; d = 3.26; 2.82; 1.99; 1.63 Å for 2θ = 27.35°; 31.68°; 45.43°; 56.44°, respectively.

higher value. DTA and TGA curves (results not shown) indicated that $FePO_{4(am)}$ and $FePO_{4(cr)}$ maximal thermal stability temperature are respectively 656 and 613 °C. Solids were therefore stable under our experimental conditions. Mass losses corresponding to dehydration (at around 150 °C) were respectively 21% for $FePO_{4(am)}$ and 31% for $FePO_{4(cr)}$. The observed thermal behaviour compares well with literature data [13,17].

3.2. Adsorption experiments

Equilibrium was obtained for As(III) and As(V) after 10 h, for both $FePO_{4(am)}$ or $FePO_{4(cr)}$ (results not shown). Adsorption curves (Fig. 2) showed that As(III) was always better removed than As(V), and that maximal adsorption capacity was slightly better for $FePO_{4(am)}$: 21 mg As(III)/g $FePO_{4(am)}$ (0.28 ± 0.01 mmol/g) and 16 mg As(III)/g $FePO_{4(cr)}$ (0.21 ± 0.01 mmol/g). For As(V), adsorption was similar on both iron phosphates: 10 mg As(V)/g $FePO_{4(am)}$ (0.13 ± 0.01 mmol/g) and 9 mg As(V)/g $FePO_{4(cr)}$ (0.12 ± 0.01 mmol/g). Both solid surface state and surface charge can explain this difference: the more the solid is crystallised, the smaller the specific surface area is and the less arsenic is adsorbed. During these experiments, there were pH variations which could indicate a difference between As(III) and As(V) retention mechanisms: pH decreased by ca. 2 units for As(III) (from pH 7–9 to pH 5–7) and by ca. 0.8 units for As(V) (from pH 6–7.5 to pH 5–7).

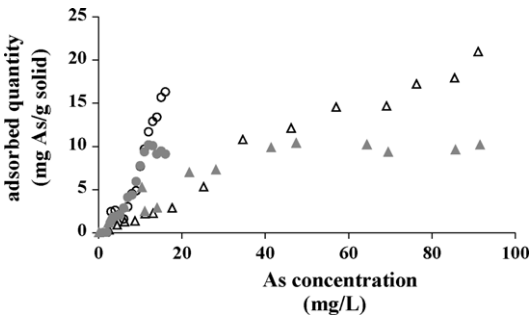

Fig. 2. Adsorption curves on $FePO_{4(am)}$ (△, ▲) and $FePO_{4(cr)}$ (◯, ●). Open symbols represent As(III) and closed symbols As(V). Experimental conditions: equilibrium time 10 h, solid concentration 1 g/L.

4. Discussion

In order to identify the retention process, phosphate, iron(II) and iron(III) release during arsenic removal were measured. The observed trends were different (Figs. 3–6). Phosphate release increased with the amount of adsorbed arsenic and this trend was more marked in the case of As(V) (Fig. 3). For both crystalline and amorphous $FePO_4$, the maximum phosphate release was reached at the highest arsenic adsorption. This result points out the probable exchange between arsenate and phosphate due to their similar ionic radii (AsO_4^{3-}: 248 nm; PO_4^{3-}: 238 nm; [18]).

Blank studies without As (i.e. solid dissolution only) gave lower phosphate release ($\ll$1 mg/L); thus the higher concentration in the case of As(III) points another phenomenon. Under our experimental pH conditions, As(III) was present as $H_3AsO_3^0$; therefore these results can suggest As(III) oxidation to As(V) followed by an arsenate/phosphate exchange.

During As(III) adsorption onto $FePO_{4(am)}$, Fe(III) reached a constant value (Fig. 5) whereas Fe(II) reached a maximum then decreased (Fig. 4); this can corroborate As(III) oxidation by Fe(III). During As(V) adsorption, Fe(III) release followed the same trend as As(III), but with a higher maximum (Fig. 6).

There was almost no Fe(II) release (<1 mg/L) during As(V) adsorption onto $FePO_{4(am)}$ or $FePO_{4(cr)}$ (results not shown) which confirms As(III) oxidation.

During adsorption on $FePO_{4(cr)}$, Fe(II) and Fe(III) trends and concentrations were the same as those previously observed on $FePO_{4(am)}$ (results not shown); yet, maximal iron concentrations released during adsorption were reached for higher initial arsenic concentrations.

4.1. Precipitation of iron(II) arsenate

Iron(II) release was observed only during As(III) adsorption, which confirms As(III) oxidation by iron(III):

$$Fe^{3+} + 1e^- \Leftrightarrow Fe^{2+}$$

$$E = 0.770 + 0.059 \log \frac{[Fe^{3+}]}{[Fe^{2+}]}$$

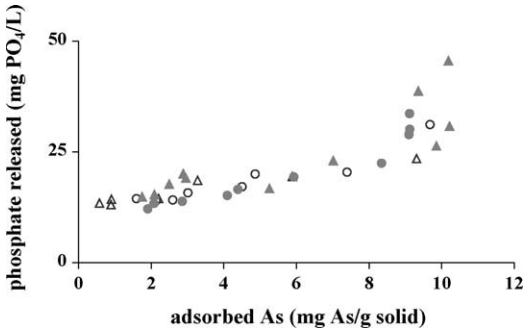

Fig. 3. Phosphate release during retention on $FePO_{4(am)}$ (△, ▲) and $FePO_{4(cr)}$ (◯, ●). Open symbols represent As(III) and closed symbols As(V). Solid concentration is 1 g/L.

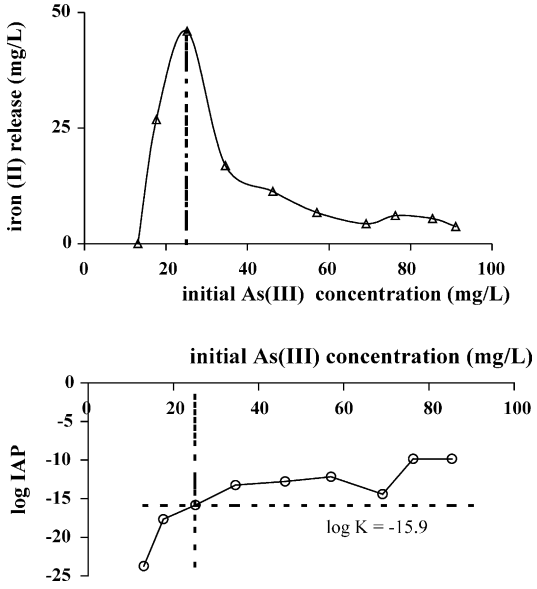

Fig. 4. Iron(II) release (△) during As(III) retention on $FePO_{4(am)}$ and corresponding log IAP (◯).

$$H_3AsO_3{}^0 + 2H_2O \Leftrightarrow HAsO_4{}^{2-} + 4H^+ + 2e^-$$

$$E = 0.881 - 0.1182pH + 0.0295 \log \frac{[HAsO_4{}^{2-}]}{[H_3AsO_3]}$$

where E is the Nernst redox potential (V), calculated at 25 °C [19].

This oxidation leads to the release of Fe^{2+} ions which can precipitate with arsenate:

$$3Fe^{2+} + 2HAsO_4{}^{2-} \Leftrightarrow Fe_3(AsO_4)_2 + 2H^+$$

with

$$K = \frac{[Fe^{2+}]^3[HAsO_4{}^{2-}]^2}{[H^+]^2}$$

where $K = 10^{-15.9}$ [20] for $Fe_3(AsO_4)_2{\cdot}8H_2O_{(s)}$.

The possible formation of this precipitate during our experiments was assessed by calculating the ion activity product IAP for each initial arsenic and iron(II) concentration as follows:

$$IAP = \frac{[Fe(II)_{total}]^3}{\alpha^3_{Fe(II)}} \frac{[As_{total}]^2}{\alpha^2_{As}[H^+]^2}$$

where the α coefficients take into account the pH influence on speciation [21]. All IAP calculations were computed with the MINEQL+ speciation software [22], using the equilibrium constants dataset from Morel and Hering [23].

It is clear that for both $FePO_{4(am)}$ or $FePO_{4(cr)}$, the precipitation of iron(II) arsenate was thermodynamically favoured ($\log IAP > \log K$) for an initial arsenite concentration greater than 25 ± 1 mg/L (Fig. 4). This meant that the beginning of the precipitation may have occurred when iron(II) concentration, during As(III) retention, was at and above the maximal value. Maximal iron(II) release was a little higher when considering adsorption on $FePO_{4(am)}$, and the decrease was greater. This could indicate an increased precipitation when As(III) was adsorbed onto $FePO_{4(am)}$, which also explains the highest arsenic removal capacity when using this sorbent.

4.2. Precipitation of iron(III) arsenate

Iron(III) and phosphate release can be explained by solid dissolution and arsenate/phosphate substitution. The presence in solution of both iron(III) due to dissolution ($-\log K_s = 26.4$ for $FePO_4$ [23]) and arsenate due to As(III) oxidation could lead to the precipitation of $FeAsO_{4(s)}$ as follows:

$$Fe^{3+} + HAsO_4{}^{2-} \Leftrightarrow FeAsO_4 + H^+$$

with

$$K = \frac{[Fe^{3+}][HAsO_4{}^{2-}]}{[H^+]}$$

where $K = 10^{-11.7}$ [20] for $FeAsO_4{\cdot}2H_2O_{(s)}$ (scorodite).

The possible formation of this precipitate during our experiments was assessed as previously by calculating the ion activity product IAP for each initial arsenic and iron(III) concentration:

$$IAP = \frac{[Fe(III)_{total}][As_{total}]}{\alpha_{Fe(III)}\alpha_{As}[H^+]}$$

Results (Fig. 5) showed that the precipitate is thermodynamically favoured ($\log IAP > \log K$) for As(III) concentrations above 20 ± 1 mg As/L, yet the precipitate between Fe(II) and As(V) was more likely to occur as the decreasing trend seemed more marked.

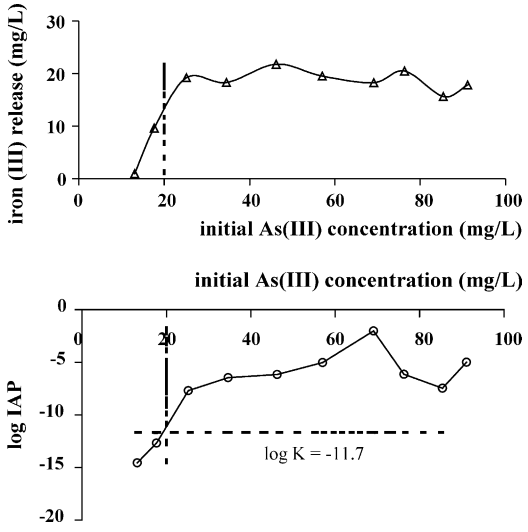

Fig. 5. Iron(III) release (△) during As(III) retention on $FePO_{4(am)}$ and corresponding log IAP (◯).

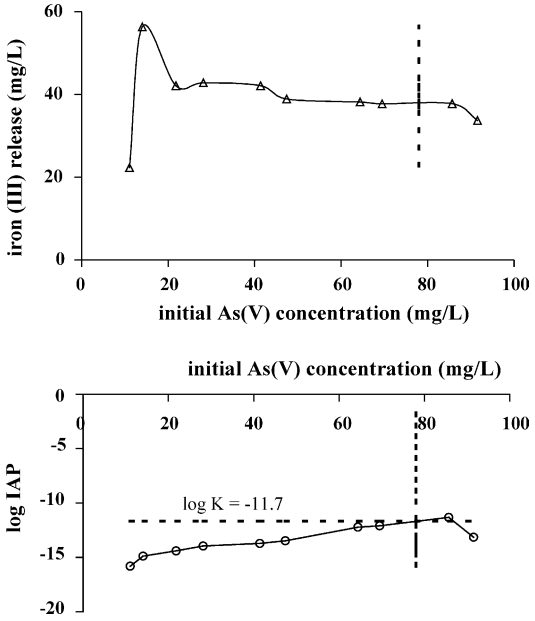

Fig. 6. Iron(III) release (△) during As(V) retention on $FePO_{4(am)}$ and corresponding log IAP (◯).

Based on Fe(III) release during As(V) adsorption on $FePO_{4(am)}$ and $FePO_{4(cr)}$, the precipitation of $FeAsO_4 \cdot 2H_2O_{(s)}$ can also be considered during As(V) adsorption onto iron phosphate. IAP calculations were performed in the same way. Results (Fig. 6) showed that precipitate formation was not thermodynamically favoured ($\log IAP < \log K$), except for high initial As(V) concentrations.

The precipitation reaction also explains the greater decrease in pH with As(III), as precipitation leads to proton release.

Phosphate release during experiments was always above 10 mg PO_4^{3-}/L, and iron release concentration was around 50 mg Fe/L. According to the European Directive 98/83/CE, phosphate and iron concentration in industrial waste water to be discharged in natural waters must not exceed 10 mg P/L (or 31 mg PO_4^{3-}/L) and 5 mg Fe/L. Therefore, iron(III) phosphate could be applied in such a case, providing iron removal techniques are considered.

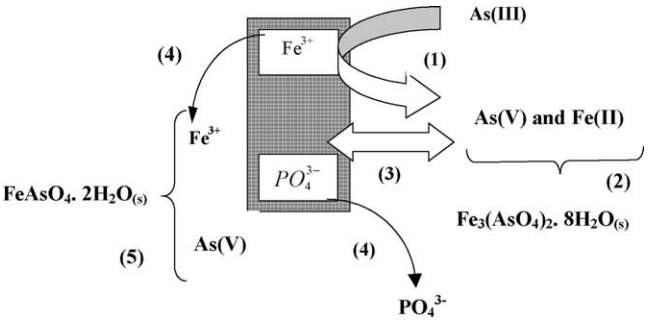

Fig. 7. Various processes involved in As retention by $FePO_4$.

5. Conclusion

Both amorphous and crystalline iron(III) phosphate are efficient at arsenic removal and various processes may be involved as summarized in Fig. 7:

- concerning As(III): (1) oxidation by Fe(III); (2) Fe(II) release and As(V) presence leading to the precipitation of $Fe_3(AsO_4)_2 \cdot 8H_2O_{(s)}$; As(V) can also substitute for PO_4^{3-} (3). At the solid surface, due to dissolution equilibrium, Fe^{3+} and PO_4^{3-} are released into solution (4) and $FeAsO_4 \cdot 2H_2O_{(s)}$ can thus precipitate (5).
- concerning As(V): phosphate substitution (3) and solid dissolution (4) lead to Fe^{3+} and PO_4^{3-} release into solution. Arsenic can also be removed by the precipitation (5) of $FeAsO_4 \cdot 2H_2O_{(s)}$ for high arsenic concentrations.

This solid would thus appear to be an interesting sorbent, although the high release of phosphate and iron will exclude its application in drinking water plants. However, this mineral can be a potential candidate for industrial waste treatment (acid mine drainage, etc.) or also for polluted soils remediation.

Acknowledgements

This work was financially supported by the “Contrat de plan Etat - Région Limousin” and by the “Conseil Régional du Limousin”.

References

[1] J. Matschullat, Arsenic in the geosphere – a review, Sci. Total Environ. 249 (2000) 297–312.
[2] P.L. Smedley, D.G. Kinniburgh, A review of the source, behaviour and distribution of arsenic in natural waters, Appl. Geochem. 17 (2002) 517–569.
[3] A.J. Bednar, J.R. Garbarino, I. Ferrer, D.W. Rutherford, R.L. Wershaw, J.F. Ranville, T.R. Wildeman, Photodegradation of roxarsone in poultry litter leachate, Sci. Total Environ. 302 (2003) 237–245.
[4] S. Lebow, R.S. Williams, P. Lebow, Effect of simulated rainfall and weathering on release of preservative elements from CCA treated wood, Environ. Sci. Technol. 37 (2003) 4077–4082.
[5] M. Masud Karim, Arsenic in groundwater and health problems in Bangladesh, Water Res. 34 (2000) 304–310.
[6] B.K. Mandal, K.T. Suzuki, Arsenic round the world: a review, Talanta 58 (2002) 201–235.
[7] E. Lombi, W.W. Wenzel, R.S. Sletten, Arsenic adsorption by soils and iron-oxide-coated sand: kinetics and reversibility, J. Plant. Nutr. Soil. Sci. 162 (1999) 451–456.
[8] J.T. Van Elteren, V. Stibilj, Z. Slejkovec, Speciation of inorganic arsenic in some bottled Slovene mineral waters using HPLC–HGAFS and selective coprecipitation combined with FI-HGAFS, Water Res. 36 (2002) 2967–2974.
[9] A. Courtin-Nomade, C. Neel, H. Bril, M. Davranche, Trapping and mobilisation of arsenic and lead in former mine tailings – environmental conditions effects, Bull. Soc. Geol. Fr. 173 (2002) 479–485.
[10] Y.W. You, H.T. Zhao, G.F. Vance, Removal of arsenite from aqueous solutions by anionic clays, Environ. Technol. 22 (2001) 1447–1457.

[11] J.A. Wilkie, J.G. Hering, Adsorption of arsenic onto hydrous ferric oxide: effects of adsorbate/adsorbent ratios and co-occurring solutes, Colloids Surf. A 107 (1996) 97–110.
[12] M.F. Hughes, Arsenic toxicity and potential mechanisms of action, Toxicol. Lett. 133 (2002) 1–16.
[13] Y. Song, S. Yang, P.Y. Zavalij, M.S. Whittingham, Temperature-dependent properties of $FePO_4$ cathode materials, Mater. Res. Bull. 37 (2002) 1249–1257.
[14] M. Davranche, S. Lacour, F. Bordas, J.-C. Bollinger, An easy determination of the surface chemical properties of simple and natural solids, J. Chem. Educ. 80 (2003) 76–78.
[15] Afnor, Evaluation de la Qualité des Sols, vol. 1: Méthodes d'Analyses Chimiques, norme NF X31-130, Détermination de la CEC, Afnor édition, Paris. 2004, pp. 131–145 (see pp. 140–143).
[16] Afnor, Qualité de l'Eau, vol.3: Eléments Majeurs, Autres Eléments et Composés Minéraux, norme NF EN 1189, Dosage du Phosphore, 6° édition, Afnor édition, Paris, 2001, pp. 355–381.
[17] S. Scaccia, M. Carewska, A. Di Bartolomeo, P.P. Prosini, Thermoanalytical investigation of iron phosphate obtained by spontaneous precipitation from aqueous solutions, Thermochim. Acta 383 (2002) 145–152.
[18] Y. Marcus, Ion Properties, Marcel Dekker, New York, 1997.
[19] M. Pourbaix, Atlas des Equilibres Electrochimiques à 25 °C, Gautier-Villars, Paris, 1963.
[20] M. Sadiq, A. Locke, G. Spiers, D.A.B. Pearson, Geochemical behaviour of arsenic in Kelly Lake, Ontario, Water Air Soil Pollut. 141 (2002) 299–312.
[21] A. Ringbom, Complexation in Analytical Chemistry, Wiley, New York, 1963.
[22] W.D. Schecher, D.C. McAvoy, MINEQL+: A Chemical Equilibrium Modeling System, version 4.0 for Windows, Environmental Research Software, Hallowell ME, 1998.
[23] F.M.M. Morel, J.G. Hering, Principles and Applications of Aquatic Chemistry, Wiley, New York, 1993.